In vivo detection of macrophages in a rabbit atherosclerotic model by time-resolved laser-induced fluorescence spectroscopy

Laura Marcu [a,b,*], Qiyin Fang [a], Javier A. Jo [a], Thanassis Papaioannou [a],
Amir Dorafshar [c], Todd Reil [c], Jian-Hua Qiao [e], J. Dennis Baker [c],
Julie A. Freischlag [d], Michael C. Fishbein [e]

[a] *Biophotonics Research & Technology Development, Department of Surgery, Cedars-Sinai Medical Center,
8700 Beverly Blvd., G149A Los Angeles, CA 90048, USA*
[b] *Departments of Biomedical and Electrical Engineering/Electrophysics, University of Southern California, Los Angeles, CA, USA*
[c] *Department of Vascular Surgery, David Geffen-UCLA School of Medicine, Los Angeles, CA, USA*
[d] *Department of Surgery, Johns Hopkins University School of Medicine, Baltimore, MD, USA*
[e] *Department of Pathology and Laboratory Medicine, David Geffen-UCLA School of Medicine, Los Angeles, CA, USA*

Abstract

Accumulation of numerous macrophages in the fibrous cap is a key identifying feature of plaque inflammation and vulnerability. This study investigates the use of time-resolved laser-induced fluorescence spectroscopy (TR-LIFS) as a potential tool for detection of macrophage foam cells in the intima of atherosclerotic plaques. Experiments were conducted in vivo on 14 New Zealand rabbits (6 control, 8 hypercholesterolemic) following aortotomy to expose the intimal luminal surface of the aorta. Tissue autofluorescence was induced with a nitrogen pulse laser (337 nm, 1 ns). Lesions were histologically classified by the percent of collagen or macrophage foam cells as well as thickness of the intima. Using parameters derived from the time-resolved fluorescence emission of plaques, we determined that intima rich in macrophage foam cells can be distinguished from intima rich in collagen with high sensitivity (>85%) and specificity (>95%). This study demonstrates, for the first time, that a time-resolved fluorescence-based technique can differentiate and demark macrophage content versus collagen content in vivo. Our results suggest that TR-LIFS technique can be used in clinical applications for identification of inflammatory cells important in plaque formation and rupture.
© 2005 Elsevier Ireland Ltd. All rights reserved.

Keywords: Time-resolved fluorescence spectroscopy; Atherosclerotic diagnosis; Vulnerable plaques

1. Introduction

Atherosclerosis develops through a progressive process that is largely characterized by accumulation of lipids and fibrous constituents in the arterial wall. This results in stenosis and reduction of blood flow [1,2]. Over the past decade significant progress has been made in defining the cellular and molecular interactions involved in the process of atherogenesis as well as in the understanding of mechanisms leading to

clinical complications [1–6]. It is now clear that the risk of an acute clinical event, such as sudden plaque rupture with subsequent thrombosis, depends primarily on the composition and "vulnerability" of the plaque rather than the severity of stenosis. Chronic inflammatory conditions within the blood vessel can result in the weakening and rupture of the plaque fibrous cap and is associated with clinical complication resulting in either myocardial infarction or stroke [1–6].

Generally, differentiation of monocytes into macrophages associated with accumulation of highly oxidized aggregate low-density-lipoprotein (LDL) within the intima results in the formation of foam cells that will trigger inflammation

---

* Corresponding author. Tel.: +1 310 423 8077; fax: +1 310 423 8414.
E-mail address: lmarcu@bmsrs.usc.edu (L. Marcu).

and weakening of the structural integrity of the fibrous cap. In addition, macrophages produce proteolytic enzyme that digest extracellular matrix proteins in the fibrous cap that further enhance this process [1–6]. As recently acknowledged in a consensus document [7], vulnerable plaques generally have thin fibrous caps and increased numbered of inflammatory cells. Rupture typically occurs at the lesion edges that are rich in inflammatory cells [1–7]. Thus, detection of inflammation was identified as a major criterion for diagnosis of "vulnerable" plaques. Atherosclerotic plaques with active inflammation demonstrate extensive macrophage accumulation [7–9]. Consequently, techniques that can detect macrophages in vivo are needed to assess the risk of plaque complication. A set of imaging tools [7,10–12] have been identified as potential diagnostic techniques for plaque vulnerability. These include intravascular techniques such as thermography [13,14], contrast-enhanced MRI [15,16], fluorodeoxyglucose positron emission tomography [17,18], immunoscintigraphy [19] and optical coherence tomography (OCT) [8,20]. For the studies reported here, we hypothesized that in addition, time-resolved laser-induced fluorescence spectroscopy (TR-LIFS) could represent an alternative or synergetic approach for detection of fibrous cap rich in macrophages or other inflammatory cells.

Fluorescence spectroscopy-based techniques, including steady-state (spectrally resolved) and time-resolved approaches, have been shown to detect elastin, collagen, lipids and other sources of autofluorescence in normal and diseased arterial walls as well as to characterize the biochemical composition of atherosclerotic plaques both ex vivo and in vivo. These techniques and applications have been comprehensively reviewed elsewhere [21–23]. In the context of "vulnerable" plaque diagnosis, a few studies have reported the application of fluorescence techniques to the identification of plaque disruption [24], detection of plaques with thin fibrous cap [25] and discrimination of lipid-rich lesions [26]. Nevertheless, to the best of our knowledge, the detection of macrophages/foam cells infiltration in atherosclerotic artery wall using fluorescence spectroscopy techniques has not been reported.

Extending on our previous work [22,26], conducted on human carotid and aortic specimens, and tailored to staging of plaque based upon their composition and to identification of lipid-rich lesions, this study investigated the ability of TR-LIFS as tool for the in vivo detection of macrophages in the arterial intima. We employed a rabbit atherosclerotic model, previously used in the quantification of macrophage content in plaques by OCT [8] and a clinically compatible TR-LIFS apparatus [27] that allowed for collection and analysis of both spectrally and temporally resolved fluorescence emission spectra. The goals of this study were: (i) to determine fluorescence-derived parameters that allow discrimination between atherosclerotic intima rich in macrophages, from intima rich in collagen (fibrous tissue); and (ii) to evaluate the accuracy of this technique for predicting macrophage accumulation in the fibrous cap.

2. Methods and materials

2.1. Atherosclerotic animal model

Twelve male New Zealand white rabbits (10–15 lbs body weight) were used in this study. The animals were housed in the vivarium facilities of the Health Sciences Center at the University of California at Los Angeles (UCLA) under the current guidelines of the NIH. After a 2 week quarantine, the rabbits were divided in two groups and fed either a high cholesterol diet (0.3% cholesterol) (eight animals—atherosclerotic group) for at least 8 weeks prior to study, or a normal Prolab® (LabDiet, St. Louis, MO) rabbit diet (six animals, control group). Prior to TR-LIFS studies, the animals were anaesthetized with IM injections of ketamine (10 mg/kg) and isopromazine (0.2 mg/kg). A tracheotomy was performed for mechanical ventilation during the procedure. Angiocatheters (18-French) were inserted into the right common carotid artery to monitor the systemic arterial pressure and to measure arterial blood gases. Body temperature was maintained with a heating pad set at 37 °C and monitored with a rectal temperature probe. A midline sternotomy and laparotomy were performed to expose the thoracic and abdominal aorta. The entire thoracoabdominal aorta was exposed and all branches ligated with silk sutures to exclude the aorta. A longitudinal aortotomy was then made to expose the intimal luminal surface of the aorta. TR-LIFS data were collected from this surface. After spectroscopic investigations, the animals underwent euthanasia, then arterial segments from where data were collected were removed for histological analysis.

2.2. TR-LIFS measurements—in vivo

The in vivo measurements were conducted with an experimental TR-LIFS prototype apparatus (Fig. 1), recently developed by our group [27] that allowed for spectrally resolved fluorescence lifetime measurements. Briefly, autofluorescence of tissue was induced with a pulsed nitrogen laser (Lasertechnik Berlin, Berlin, Germany, model MNL200-ATM205, wavelength 337 nm, pulse width 700 ps, frequency 30 Hz) using a custom made sterilizable bifurcated fiber-optic probe (CeramOptec, East Longmeadow, MA). The probe consisted of a central excitation tapered fiber-optic (diameter 600 μm, numerical aperture 0.11) surrounded by a collection ring of 12 fibers (diameter 200 μm, numerical aperture 0.22). The source–detector separation, center-to-center, was 480 μm. The laser excitation pulse width measured at the tip of the fiber was 1 ns full width at half maximum. The collected fluorescence was dispersed by an imaging spectrometer/monochromator (Chromex Inc., Albuquerque, NM, model 250 is/sm, F/4.4, 600 g/mm grating, blazed at 450 nm) and detected with a gated multi-channel plate photo-multiplier tube (MCP-PMT Hamamatsu, Bridgewater, NJ, model R5916-50; rise time 180 ps). The
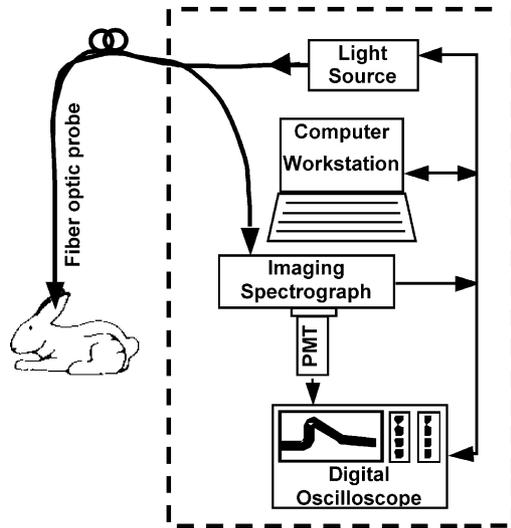
Fig. 1. Schematic representation of the TR-LIFS apparatus. The fiber-optic probe enabled remote delivery of the excitation light to and collection of the fluorescence emission from the rabbit aorta as exposed through the midline sternotomy and laparotomy. *Note:* In future clinical implementation, the fiber-optic probe can be integrated in any of the conventional catheter-based techniques currently used for the interrogation of arterial vessels including angioscopes and intravascular ultrasound catheters.

fluorescence was temporally resolved using a digital phosphor oscilloscope (TDS5104, Tektronix, Beaverton, OR; bandwidth 1 GHz, sampling rate 5 Gsamples/s) coupled to a preamplifier (Hamamatsu, Bridgewater, NJ, model C5594; bandwidth 1.5 GHz). A long pass filter (360 nm) was used to remove the scattered excitation light (337 nm) from the detection path. The laser triggering, wavelength scanning and data acquisition, storage and processing were controlled using a computer workstation and custom analytical software written in LabVIEW (National Instruments, Austin, TX) and MATLAB (Mathwork, Inc). Overall, for the TR-LIFS measurements reported in this study, the time-resolved spectra were acquired with a spectral resolution of 5 nm, time-resolution of 300 ps and at a scanning speed of 0.8 s per wavelength.

The fiber-optic probe was placed perpendicular to the intimal surface of the aorta and held in position with a specially designed metallic holder that allow three-dimensional fine adjustments of the probe's position with respect to the interrogated tissue. The time-resolved emission measurements were obtained by serial scanning of the monochromator across a spectral range from 360 to 600 nm in increments of 5 nm. At each wavelength, 16 fluorescence pulses were collected and averaged by the oscilloscope. To assess the fluorescence lifetime reproducibility, five consecutive measurements were conducted at two wavelengths: 390 and 450 nm. The total acquisition time across the scanned emission spectrum, including the consecutive measurements, was about 37 s. After each measurement sequence, the monochromator was tuned to a wavelength slightly below the excitation laser line. The laser pulses reflected by the sample were measured and used to

represent the temporal profile of the laser pulse. This profile was later used as input to the deconvolution algorithm for the estimation of fluorescence lifetimes. Laser excitation output measured at the tip of the probe was set at 2 μJ/pulse (fluence 1.8 μJ/mm^2 per pulse, fluence rate 54 μW/mm^2 at the tissue level). This output was found to be a reasonable compromise between an adequate signal-to-noise ratio and the photobleaching of the sample [28]. To minimize the motion artifacts due to cardiac cycle and breathing, the investigated aortic sections were gently stabilized with a plastic clamp. Blood interference was kept at minimum with saline irrigation as well as occasional application of surgical clamps to distal or proximal area. The TR-LIFS data were recorded from regions visually identified as either normal or atherosclerotic plaques situated in abdominal and thoracic areas (15—normal control group; 72—atherosclerotic group).

2.3. Histological analysis

Following in vivo acquisition, all spectroscopically investigated aortic areas/segments were removed, fixed (10% buffered formalin), processed routinely and embedded in paraffin. Two sequential 4-μm-thick sections were cut from each segment and stained with hematoxylin and eosin (H&E) and a combined trichrome/elastin method, respectively. Each section was evaluated by light microscopy for elastin, collagen and macrophage content. Intima and media thicknesses were measured from the digitized pictures of the histological slides using the AxioVision image processing software (Carl Zeiss Inc., Germany). Each digitized picture was further evaluated for the composition of artery wall. Macrophages were identified in the H&E stained sections as cells with small, usually central round nuclei, with abundant, surrounding foamy to granular cytoplasm. Macrophage could be also seen in the trichrome/elastin stained slides as small cells with dark round nuclei and clear cytoplam. Mature collagen stained blue, elastin stained black and smooth muscle cells stained red in the trichrome/elastin stained sections. Both the intimal wall thickness and the density of the macrophages and collagen in the intima were evaluated in several randomly selected regions per transverse section by two cardiovascular pathologists. The lesions were classified in six categories based on the overall histological characteristics (normal versus atherosclerotic), composition (percent of collagen versus percent of macrophage content) and thickness (thin versus thick) of the intima as follows: normal-control group (N-Control), normal-atherosclerotic group (N-Athero), thin lesion collagen rich (Thin-Collagen), thin lesion macrophage rich (Thin-Mac), thick lesion collagen rich (Thick-Collagen) and thick lesion macrophage rich (Thick-Mac). The lesions with the intima thickness less than 50 μm were defined as "Thin", the lesions with collagen content greater than 50% and macrophage content less than 20% were defined as "collagen"-rich and the lesions with macrophage content larger than 20% and collagen content smaller than 50% were defined as "foam"-rich.

2.4. TR-LIFS data analysis and statistics

The time-resolved fluorescence spectrum or the intrinsic fluorescence impulse response function (IRF), $h(n)$, was recovered by numerical deconvolution of the measured input laser pulse, $x(n)$, from the measured fluorescence response transient, $y(n)$, as given by equation:

$$y(n) = T \sum_{m=0}^{M-1} h(m)x(n-m)$$

where parameter M determines the extent of the system memory and T is the sampling interval. A Laguerre expansion technique [29,30] was used for deconvolution. The technique uses the orthonormal set of discrete time Laguerre functions $b_j^\alpha(n)$ to discretize and expand the fluorescence IRF:

$$h(n) = \sum_{j=0}^{L-1} c_j b_j^\alpha(n)$$

where c_j is the unknown Laguerre expansion coefficients (LEC), which was estimated from the input–output data by generalized linear least-square fitting, $b_j^\alpha(n)$ denotes the jth order orthonormal discrete time Laguerre function [29] and L is the number of Laguerre functions used to model the IRF. The Laguerre parameter $(0 < \alpha < 1)$ determines the rate of exponential decline of the Laguerre functions. Once the fluorescence IRF's were estimated for each emission wavelength, the steady-state spectrum (I_λ), was computed by integrating each intensity decay curve as a function of time. Further, to characterize the temporal dynamics of the fluorescence decay, two sets of parameters were used: (1) the average lifetime (τ_f) computed as the interpolated time at which the IRF decays to 1/e of its maximum value and (2) the normalized value of the corresponding LEC's $(c_j, j = 0, \ldots, L-1)$. Thus, a complete description of each sample fluorescence as a function of emission wavelength, λ_E, was given by the variation of a set of spectroscopic parameters $(I_\lambda, \tau_f$ and c_j's). This represents a new analytical approach for characterization of fluorescence decay recently developed by our research group [30].

In order to identify a set of spectroscopic parameters that will best discriminate between different tissue types, a univariate statistical analysis (one-way ANOVA) was used to compare the spectroscopic parameters $(I_\lambda, \tau_f$ and c_j's) at specific λ_E's for each type of tissue as defined by histology. A post hoc comparison test (Student–Newman–Keuls) was used to complement the results of the ANOVA test. A P-value of <0.05 was assumed to indicate statistical significance. All the results are presented as mean ± standard error (S.E.). The results of this statistical analysis were used to identify significant differences among parameters that characterize each tissue type and provided a semi-empirical evaluation of those spectroscopic parameters likely to provide means of discrimination between different compositional features of the carotid plaque.

2.5. Classification

The histolopathologic classification results were used to validate the TR-LIFS results for distinct tissue categories using two classification criteria. Classification #1 was used to separate the Thick-Mac sub-group from Thick-Collagen and from N-Athero sub-groups. Classification #2 was used to distinguish Thin-Mac sub-group from Thin-Collagen and from N-Athero sub-groups. A set of intensity ratios (total of 5) at four emission wavelengths (360, 390, 450 and 500 nm) and time-resolved parameters (total of 16), values and ratios of c_j's at three emission wavelengths (390, 450 and 500 nm) were used as input predictor variables in a stepwise linear discriminant analysis algorithm (SLDA) [31]. Using a leave-one-out (cross-validation) approach, the algorithm was tested for its ability to predict the dominance of either macrophages or collagen in each sub-group type as identified in the histopathological analysis. This approach was shown to be suitable for the creation of the test set when the number of samples is small [31]. The accuracy of prediction was determined for two situations: (a) predictor variables selected only from spectrally derived parameters, "Spectral" and (b) predictor variables selected from spectrally and time-resolved-derived parameters, "Spectral&Time".

3. Results

3.1. Histology

The normal aortic segments from the N-Control group were characterized by a very thin intima composed of an endothelial cell layer and small amounts of subendothelial connective tissue, with an underlying media composed of alternative layers of elastic fibers and smooth muscle cells. The aortic areas from the atherosclerotic rabbit group were classified as N-Athero = 26 (intima thickness: below 3 μm), Thin-Collagen = 10 (median 42.2 μm), Thin-Mac = 7 (median 43.1 μm), Thick-Collagen = 16 (median 119.4 μm) and Thick-Mac = 14 (median 144.3 μm). Fig. 2 depicts representative histological sections. The N-Athero samples show similar features with those observed in N-Control samples. In the Thin- and Thick-Collagen samples the intima is thickened mainly by collagen and smooth muscle cells, while in the Thin- and Thick-Mac sample the intima is thickened primarily by macrophages and a small amount of smooth muscle cells.

3.2. Time-resolved fluorescence spectra and characteristics

Representative time-resolved fluorescence spectra of normal and rabbit atherosclerotic lesions, as retrieved using the Laguerre expansion technique and employed in the reconstruction of the conventional steady-state spectrum and the
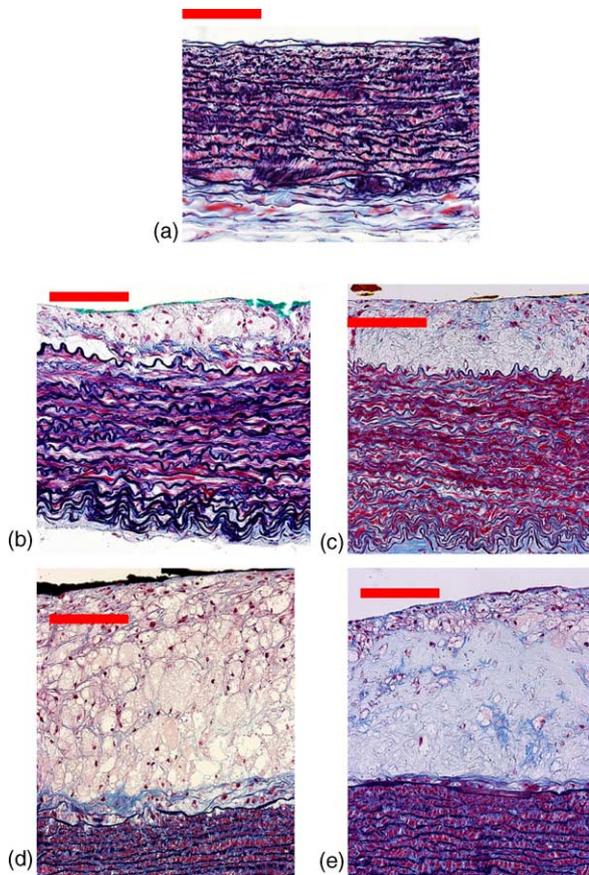
Fig. 2. Examples of aortic wall. (a) Normal (N-Athero sub-group), (b) Thin-Mac, (c) Thick-collagen, (d) Thick-Mac and (e) Thick-collagen. Scale bar 50 μm.

characterization of the intensity decay are given in Fig. 3: N-Athero (Fig. 3a), Thick-Collagen (Fig. 3b) and Thick-Mac (Fig. 3c). The normalized steady-state spectrum of each type of the tissue sample is depicted in Fig. 2c. Each sample was defined by a relatively broad-band emission (two peaks: main peak at ∼385–395 nm and a second peak at ∼440–450 nm) and modulated by a valley at 415 nm. The valley corresponds to the hemoglobin absorption as previously reported [32]. The largest broad-band emission spectrum was recorded for the N-Athero and Thin-Collagen samples (main peak at about 395 nm, ∼80% of the main peak at 440 nm). The emission of the Thick-Collagen and Thick-Mac lesions was found narrow broadband with a lightly blue-shifted main peak emission (∼385 nm) and low intensities values (∼50% of the main peak at 440 nm). The emission intensity of the Thin-Mac sub-group at 440 nm averaged ∼65% of the main peak intensity.

The characteristics of fluorescence intensity decay are shown in Fig. 3e–g. For the wavelength range below 400 nm, the average radiative lifetimes values were found to be similar for all tissue types, ranging from about 1.8 to 2 ns (Fig. 3e). The lifetime values (380 nm) were slightly larger for Thick-Collagen (2.04 ± 0.05) and Thick-Mac (2.03 ± 0.05) lesions when compared with the N-Athero (1.89 ± 0.02) and Thin-Collagen (1.95 ± 0.05) sub-groups. The lifetime

values diminished gradually with the increased emission wavelength for all samples. However, the rate of lifetime values decrease was found tissue-type dependent. The shortest lifetime values and the steepest decrease of lifetime values with increased wavelength were recorded for the thick-macrophages samples. For example at 500 nm emission, the fluorescence lifetime of Thick-Mac tissue sub-group was significant lower ($\tau_{\lambda=500} = 1.41 \pm 0.04$) than that retrieved for Thick-Collagen (1.58 ± 0.04), Thin-Mac (1.53 ± 0.05), Thin-Collagen (1.68 ± 0.02) and N-Athero (1.72 ± 0.02) samples. Along the emission wavelengths, the Laguerre expansion coefficients of zero-order, LEC-0 (Fig. 3e), followed trends that were similar with those of the lifetime values (Fig. 3f). While the Laguerre coefficients of first-order, LEC-1 (Fig. 3g), revealed opposite trends. The minimal variation of LEC-1 with wavelength was observed for the Thick-Mac samples. Table 1 summarizes the values of main spectroscopic parameters from both spectral- and time-domain that allow discrimination between distinct types of tissues. Overall the spectroscopic characteristics of N-Control samples were found similar with those of the N-Athero samples (data not shown).

3.3. Classification

The two-dimensional scatterplot of two discriminant functions used to separate (a) Thick-Mac samples from Thick-Collagen and N-Athero samples and (b) Thin-Mac samples from Thin-Collagen and N-Athero samples are given in Fig. 4a and b, respectively. The functions were constructed using predictor variables derived from both spectral-resolved (ratios of intensity at discrete emission wavelengths) and time-resolved (values of fluorescence lifetimes values and values and ratios of Laguerre expansion coefficients at discrete emission wavelengths) domains. The predictor variables identified to account for more than 90% of the variance were (I_{390}/I_{450}, I_{390}/I_{360}, I_{450}/I_{360}, LEC-0_{500}, LEC-1_{450}, LEC-2_{500}/LEC-2_{390}, LEC-3_{390}) in the first case and (I_{390}/I_{450}, LEC-2_{500}/LEC-2_{390}) in the second case. Table 2 summarizes the classification results (leave-one-out approach) for the two situations "Spectral" and "Spectral&TR". The overall classification accuracy has improved when both spectral and time-resolved features were used to build the discriminant algorithm from 76.8% ("Spectral") to 92.9% ("Spectral&TR").

4. Discussion

This study demonstrates that TR-LIFS can be used to identify macrophage infiltration in the fibrous cap, a key marker of plaque inflammation, and thus targets one of the major criteria for detection of histological features associated with plaque vulnerability. Using parameters derived from the time-resolved fluorescence emission of plaques measured in vivo in a rabbit atherosclerotic model, we determined that intima rich in macrophages can be distinguished from intima
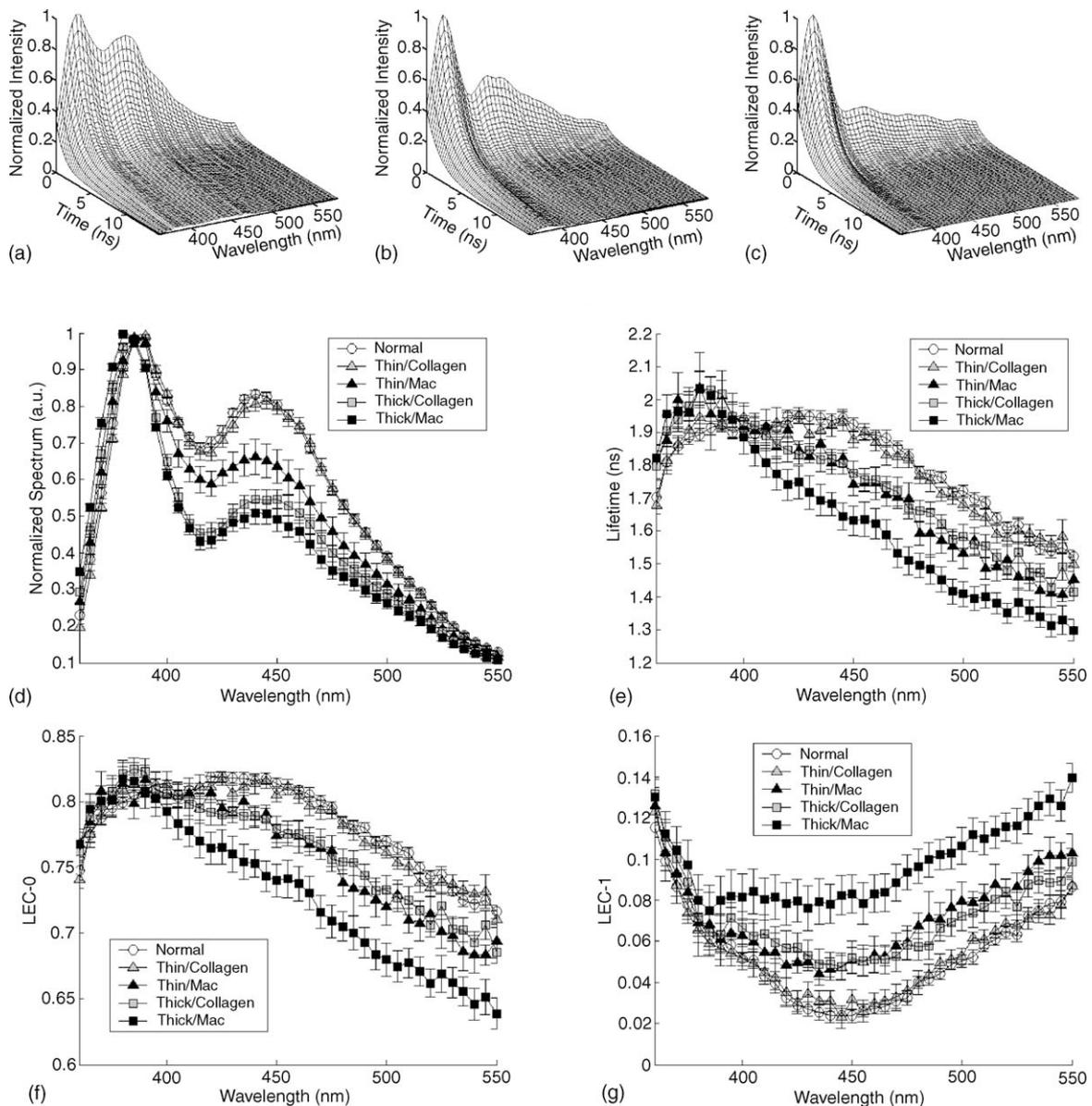
Fig. 3. Representative time-resolved fluorescence spectra or IRF of the (a) N-Athero aortic wall, (b) Thick-Collagen lesions and (c) Thick-Mac lesions. Spectroscopic features retrieved from the IRFs of each tissue group: (d) normalized spectrum, (e) fluorescence lifetime (τ_f), (f) Laguerre coefficients of zero-order (LEC-0) and (g) Laguerre coefficients of first-order (LEC-1). Data are given as mean ± S.E.

rich in collagen with high sensitivity (>85%) and specificity (>95%). While it has been reported [32–37] that fluorescence spectroscopy is sensitive to atherosclerotic plaque composition including identification of atherosclerotic plaques with thin fibrous cap [25] and lipid-rich pools [22,26], this study demonstrates, for the first time, that a fluorescence-based technique is also sensitive to differences in macrophage content versus collagen content.

Table 1
Representative set of spectroscopic parameters that allow tissue sub-groups discrimination

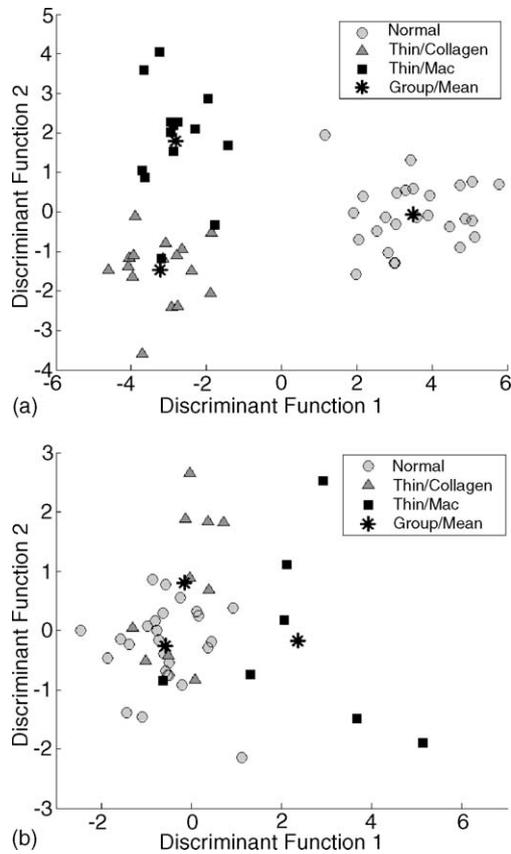|	N-Athero	Thin-Collagen	Thin-macrophage	Thick-Collagen	Thick-macrophage
I_{450}/I_{360}	1.19 ± 0.02	1.22 ± 0.03	1.56 ± 0.16	1.86 ± 0.09	2.00 ± 0.12
LEC-0$_{500}$	0.768 ± 0.003	0.760 ± 0.003	0.725 ± 0.012	0.730 ± 0.009	0.679 ± 0.012
LEC-1$_{450}$	0.024 ± 0.003	0.026 ± 0.005	0.049 ± 0.005	0.049 ± 0.007	0.081 ± 0.009
LEC-2$_{500}$/LEC-2$_{390}$	1.24 ± 0.01	1.28 ± 0.01	1.40 ± 0.03	1.47 ± 0.02	1.57 ± 0.04
LEC-3$_{390}$	0.019 ± 0.001	0.017 ± 0.001	0.011 ± 0.003	0.009 ± 0.001	0.008 ± 0.002

Fig. 4. Results of the stepwise linear discriminant analysis. Scatterplot depicts the discriminant score of the each the three tissue sub-groups: (a) N-Athero vs. Thick-Collage vs. Thick-Mac and (b) N-Athero vs. Thin-Collagen vs. Thin-Mac.

4.1. Spectroscopic characteristics and composition

Structural proteins elastin and collagen types I and III are broadly recognized as the main fluorophores in the arterial wall [22,23,26,32,33]. The fluorescence characteristics of the normal wall and thin-collagen lesions (broad emission spectrum: 360–500 nm; lifetime at peak emission region: ~1.9 ns) closely resemble the emission of elastin slightly modulated by that of collagen [22,26,32,33], thus suggesting that the elastin largely found in the media and internal elastic dominates the fluorescence emission of these two tissue sub-groups. The penetration depth of irradiation at about

Table 2
Classification accuracy (selectivity and specificity)

Group sub-type	Spectral only		Spectral and TR	
	Selectivity (%)	Specificity (%)	Selectivity (%)	Specificity (%)
N-Athero	92.3	100	96.2	100
Thick-Collagen	62.5	87.5	93.8	92.9
Thick-Foam	64.3	81.0	85.7	95.0
N-Athero	61.5	76.5	69.2	70.6
Thin-Collagen	70.0	66.7	60.0	85.7
Thin-Foam	42.9	94.4	85.7	97.2

337 nm in artery ranges between 150 and 200 μm. Thus in the current study, we expected that the thinner the lesion, the more contribution from media fluorophores (elastin in particular) to the overall fluorescence emission observed. Upon ultraviolet light excitation, elastin has a broad emission spectrum (above 70 nm half width at half maximum (HWHM), peak at ~400–410 nm) lasting (lifetime) for about 2 ns, while the collagen type I emission, for example, is blue-shifted (~385 nm), narrow (about 40 nm) and long-lasting (~4 ns) [22,38].

The increase of intima thickness due to either buildup of collagen fibers or accumulation of macrophages resulted in a narrow broad-band emission centered at about 380–390 nm and a slight lifetime (~2 ns) increase relative to normal samples. These trends suggest a strong contribution of the collagen type I fluorescence [38] to the overall emission of Thick-Collagen and Thick-Mac lesions. However, the fluorescence lifetime of these lesions was found to be wavelength-dependent. At the red-shifted wavelengths, the emission was characterized by a fast decay dynamics that appears to be associated with the accumulation of macrophage in the intima (Fig. 3), the shortest lifetimes being retrieved for the Thick-Mac lesions. Lipid components were reported to exhibit shorter-lived emission when compared to structural proteins elastin or collagen [22]. Recently, Arakawa et al. [25] reported that lipids such as cholesteryl oleate and oxidized LDL, which are a hallmark of macrophage-rich plaques, are characterized by a red-shifted fluorescence emission. Thus, our results, showing a significant decrease in lifetime primarily at longer wavelengths, are in agreement with this early work.

Our study also demonstrates that TR-LIFS allows detection of the relative changes of collagen and macrophage content in the atherosclerotic intima of our hypercholesterolemic animal model, including changes within thin atherosclerotic intima (<50 μm) underlined by media rich in elastic fibers. Although the atherosclerotic plaques in this animal model do not replicate the human atherosclerotic plaques predisposed to rupture, this finding is important, because the composition of these plaques share similarities with those of the fibrous cap covering the lipid-rich core in human vulnerable plaques [14]. The fibrous cap is typically composed [1–8] of collagen-rich matrix, relatively small number of smooth muscle cells and small number of macrophages, features that were also observed in the plaques of the hypercholesterolemic rabbits used in this study. In addition, within the same plaque thickness of this rabbit model, plaques with reduced number of macrophages and increased content of collagen can be found. Such features resemble the histological features of fibrous lesions that are likely to be more stable. Thus, this model allows studies of the characteristics of fluorescence emission from plaques with distinct macrophage versus collagen ratios but similar plaque thicknesses, which is also the case commonly seen in vulnerable fibrotic cap.

The cap itself and the lipid-rich core, however, are not present in this rabbit animal model; thus, the fluorescence

signal collected from thin lesions in our study is influenced by the fluorescent constituents of the media (elastin), rather than those found in the lipid core of a human plaque (lipid components). Since lipids, typically, are characterized by shorter-lived fluorescence when compared to elastin or collagen, current results suggest that for a human plaque, the TR-LIFS detection of increased number of macrophage can be further enhanced. Human plaques prone to rupture are characterized by a thin cap with large number of macrophages covering a lipid rich core. Thus, even shorter overall lifetimes are expected for these plaques. Albeit, studies in more complex atherosclerotic human plaques are needed to further validate this hypothesis, the current study demonstrates that TR-LIFS enables detection of inflammatory cell in atherosclerotic intima.

4.2. Time-resolved fluorescence-based plaque diagnosis

This study demonstrated that a relatively small number of spectroscopic parameters selected from a few emission wavelengths are sufficient for the discrimination of the five tissue types investigated. The use of a set of spectroscopic parameters, derived from both spectra- and time-domain, have improved the overall accuracy of detection of lesions rich in macrophage, compared to a set when only spectra-derived variables were employed. This was valid for discrimination of both Thin- and Thick-Mac cells tissue types. Although in this study we used only a small database, our results indicate that time-resolved fluorescence spectroscopy technique is robust enough to allow good detection of macrophage infiltration in arterial intima ($\sim$70% for thin-foam and $\sim$93% for thick-foam lesions). The classification accuracy may be further improved once the number of samples for each tissue type in the training set increases. Thus, our results showed that time-resolved fluorescence spectroscopy represents a potential pathway for non-destructively gaining insights into the biochemical composition of the arterial plaques and prediction of inflammatory cell infiltration in fibrous caps.

5. Conclusion

In summary, this study demonstrates that the use of time-resolved fluorescence spectroscopy enables detection of macrophage accumulation in arterial intima and thus provides a means for diagnosis of inflammatory activity and hence fibrous cap integrity. Combined information from both spectral- and time-domain improves the diagnostic value of fluorescence measurements. In addition, because TR-LIFS measures the autofluorescent properties of tissue as a diagnostic tool, such an approach would potentially have inherent advantages over the use of exogenous imaging probes. The generation of endogenous fluorescence does not require systemic or local administration of an external imaging agents. Thus, problems associated with toxicity and pharmacodynamics/kinetics of external agents would not be encountered.

Therefore, TR-LIFS is a potentially important tool for studying the contribution of inflammatory processes to atherosclerotic plaque formation, rupture and plaque response to therapeutic agents in patients.

References

[1] Lusis AJ. Atherosclerosis. Nature 2000;407:233–41.
[2] Falk E, Shah PK, Fuster V. Coronary plaque disruption. Circulation 1995;92:657–71.
[3] Maseri A, Fuster V. Is there a vulnerable plaque? Circulation 2003;107:2068–71.
[4] Libby P, Ridker PM, Maseri A. Inflammation and atherosclerosis. Circulation 2002;105:1135–43.
[5] Steinberg D. Atherogenesis in perspective: hypercholesterolemia and inflammation as partners in crime. Nat Med 2002;8:1211–7.
[6] Kereiakes DJ. The Emperor's clothes: in search of the vulnerable plaque. Circulation 2003;107:2076–7.
[7] Naghavi M, Libby P, Falk E, et al. From vulnerable plaque to vulnerable patient: a call for new definitions and risk assessment strategies: part I. Circulation 2003;108:1664–72.
[8] Tearney GJ, Yabushita H, Houser SL, et al. Quantification of macrophage content in atherosclerotic plaques by optical coherence tomography. Circulation 2003;107:113–9.
[9] Moreno PR, Falk E, Palacios IF, Newell JB, Fuster V, Fallon JT. Macrophage infiltration in acute coronary syndromes. Implications for plaque rupture. Circulation 1994;90:775–8.
[10] MacNeill BD, Lowe HC, Takano M, Fuster V, Jang IK. Intravascular modalities for detection of vulnerable plaque: current status. Arterioscler Thromb Vasc Biol 2003;23:1333–42.
[11] Moreno PR, Lodder RA, Purushothaman KR, Charash WE, O'Connor WN, Muller JE. Detection of lipid pool, thin fibrous cap, and inflammatory cells in human aortic atherosclerotic plaques by near-infrared spectroscopy. Circulation 2002;105:923–7.
[12] Fayad ZA, Fuster V. Clinical imaging of the high-risk or vulnerable atherosclerotic plaque. Circ Res 2001;89:305–16.
[13] Stefanadis C, Diamantopoulos L, Vlachopoulos C, et al. Thermal heterogeneity within human atherosclerotic coronary arteries detected in vivo: a new method of detection by application of a special thermography catheter. Circulation 1999;99:1965–71.
[14] Verheye S, De Meyer GR, Van Langenhove G, Knaapen MW, Kockx MM. In vivo temperature heterogeneity of atherosclerotic plaques is determined by plaque composition. Circulation 2002;105:1596–601.
[15] Ruehm SG, Corot C, Vogt P, Kolb S, Debatin JF. Magnetic resonance imaging of atherosclerotic plaque with ultrasmall superparamagnetic particles of iron oxide in hyperlipidemic rabbits. Circulation 2001;103:415–22.
[16] Fayad ZA, Fuster V, Nikolaou K, Becker C. Computed tomography and magnetic resonance imaging for noninvasive coronary angiography and plaque imaging: current and potential future concepts. Circulation 2002;106:2026–34.
[17] Rudd JH, Warburton EA, Fryer TD, et al. Imaging atherosclerotic plaque inflammation with [18F]-fluorodeoxyglucose positron emission tomography. Circulation 2002;105:2708–11.
[18] Lederman RJ, Raylman RR, Fisher SJ, et al. Detection of atherosclerosis using a novel positron-sensitive probe and 18-fluorodeoxyglucose (FDG). Nucl Med Commun 2001;22:747–53.

[19] Ciavolella M, Tavolaro R, Taurino M, et al. Immunoscintigraphy of atherosclerotic uncomplicated lesions in vivo with a monoclonal antibody against D-dimers of insoluble fibrin. Atherosclerosis 1999;143:171–5.

[20] Jang IK, Bouma BE, Kang DH, et al. Visualization of coronary atherosclerotic plaques in patients using optical coherence tomography: comparison with intravascular ultrasound. J Am Coll Cardiol 2002;39:604–9.

[21] Moreno PR, Muller JE. Identification of high-risk atherosclerotic plaques: a survey of spectroscopic methods. Curr Opin Cardiol 2002;17:638–47.

[22] Marcu L, Grundfest WS, Fishbein M. Time-resolved laser-induced fluorescence spectroscopy for staging atherosclerotic lesions. In: Mycek M-A, Pogue B, editors. Handbook of biomedical fluorescence. New York: Marcel Dekker; 2003.

[23] Papazoglou TG. Malignancies and atherosclerotic plaque diagnosis—is laser induced fluorescence spectroscopy the ultimate solution? J Photochem Photobiol B 1995;28:3–11.

[24] Christov A, Dai E, Drangova M, et al. Optical detection of triggered atherosclerotic plaque disruption by fluorescence emission analysis. Photochem Photobiol 2000;72:242–52.

[25] Arakawa K, Isoda K, Ito T, Nakajima K, Shibuya T, Ohsuzu F. Fluorescence analysis of biochemical constituents identifies atherosclerotic plaque with a thin fibrous cap. Arterioscler Thromb Vasc Biol 2002;22:1002–7.

[26] Marcu L, Fishbein MC, Maarek JM, Grundfest WS. Discrimination of human coronary artery atherosclerotic lipid-rich lesions by time-resolved laser-induced fluorescence spectroscopy. Arterioscler Thromb Vasc Biol 2001;21:1244–50.

[27] Fang Q, Papaioannou T, Jo JA, Vaitha R, Shastry K, Marcu L. Time-domain laser-induced fluorescence spectroscopy apparatus for clinical diagnostics. Rev Sci Instrum 2004;75:151–62.

[28] Marcu L, Grundfest WS, Maarek JM. Photobleaching of arterial fluorescent compounds: characterization of elastin, collagen and cholesterol time-resolved spectra during prolonged ultraviolet irradiation. Photochem Photobiol 1999;69:713–21.

[29] Marmarelis VZ. Identification of nonlinear biological systems using Laguerre expansions of kernels. Ann Biomed Eng 1993;21:573–89.

[30] Jo JA, Fang Q, Papaioannou T, Marcu L. Fast model-free deconvolution of fluorescence decay for analysis of biological systems. J Biomed Opt 2004;9:743–52.

[31] Duda RO, Hart PE, Stork DG. Pattern classification. New York: Wiley; 2001.

[32] Baraga JJ, Rava RP, Taroni P, Kittrell C, Fitzmaurice M, Feld MS. Laser induced fluorescence spectroscopy of normal and atherosclerotic human aorta using 306–310 nm excitation. Lasers Surg Med 1990;10:245–61.

[33] Andersson-Engels S, Johansson J, Svanberg S. The use of time-resolved fluorescence for diagnosis of atherosclerotic plaque and malignant-tumors. Spectrochim Acta Part A-Mol Biomol Spectrosc 1990;46:1203–10.

[34] Deckelbaum LI, Stetz ML, O'Brien KM, et al. Fluorescence spectroscopy guidance of laser ablation of atherosclerotic plague. Lasers Surg Med 1989;9:205–14.

[35] Morguet AJ, Gabriel RE, Buchwald AB, Werner GS, Nyga R, Kreuzer H. Single-laser approach for fluorescence guidance of excimer laser angioplasty at 308 nm: evaluation in vitro and during coronary angioplasty. Lasers Surg Med 1997;20:382–93.

[36] Bartorelli AL, Leon MB, Almagor Y, et al. In vivo human atherosclerotic plaque recognition by laser-excited fluorescence spectroscopy. J Am Coll Cardiol 1991;17:160B–8B.

[37] Richards-Kortum R, Rava RP, Fitzmaurice M, Kramer JR, Feld MS. 476 nm excited laser-induced fluorescence spectroscopy of human coronary arteries: applications in cardiology. Am Heart J 1991;122:1141–50.

[38] Maarek JM, Marcu L, Snyder WJ, Grundfest WS. Time-resolved fluorescence spectra of arterial fluorescent compounds: reconstruction with the Laguerre expansion technique. Photochem Photobiol 2000;71:178–87.